

First-principles study of structural distortions in frustrated antiferromagnet α -NaMnO₂

Z. W. Ouyang*

Wuhan National High Magnetic Field Center, Huazhong University of Science and Technology, Wuhan 430074, People's Republic of China

B. Wang

School of Physics, Huazhong University of Science and Technology, Wuhan 430074, People's Republic of China

(Received 14 April 2010; revised manuscript received 20 July 2010; published 5 August 2010)

First-principles study on structural distortions of the frustrated antiferromagnet α -NaMnO₂ has been performed by confining the distortions within ab plane of the unit cell. The calculated ratios of lattice parameters, a/b , for both triclinic and monoclinic phases are quite close to the experimental values. The stability of antiferromagnetic triclinic phase compared to the monoclinic phase, which cannot be interpreted by the total energy and density of states, is clearly illustrated by the evolution of total energy with triclinic-monoclinic structural distortion, in good agreement with recent neutron-diffraction experiments. Magnetoelastic effect and anisotropic exchange interactions of this material are also discussed.

DOI: 10.1103/PhysRevB.82.064405

PACS number(s): 71.20.-b

I. INTRODUCTION

Over the past several years, transition-metal-based oxides with the general formula ATO_2 ($A=\text{Na}$ or Li , $T=3d$ transition metals) have been widely investigated owing to a wealth of interesting behavior, such as large thermopower,¹⁻⁴ superconductivity in several hydrated compounds,^{5,6} magnetic frustration, and novel magnetic ground states.⁷⁻¹² It is generally believed that these unusual properties are intimately associated with the distinct layered crystal structure, in which magnetic T ions map out a triangular lattice network. Particularly, in the α -NaFeO₂-type triangular lattice, A and T ions occupy octahedral sites and the TO_6 octahedra form layers separated by hexagonal nets of A cations.^{11,12} The triangular arrangement of magnetic T ions forbids simultaneous minimization of the antiferromagnetic (AFM) interaction energies acting at a given site, leading to highly degenerate ground states, i.e., magnetic frustration.

Among the representatives of this family, considerable attention has been paid to α -NaMnO₂ because of its unusual crystallography and magnetism.¹³⁻²⁰ On the one hand, α -NaMnO₂ is a triangular antiferromagnet and the original α -NaFeO₂-type rhombohedral structure ($R\bar{3}m$) is distorted into monoclinic structure ($C2/m$) due to the strong Jahn-Teller effect of Mn^{3+} ions,¹⁵ resulting in lifting of geometrical frustration. This structural stability of monoclinic phase relative to rhombohedral phase was also confirmed by first-principles study.¹⁶ On the other hand, α -NaMnO₂ owns a distinct layered structure with MnO_2 layers ferromagnetically coupled along the c_m axis. This ferromagnetic (FM) coupling is very weak and evidenced by both experiments¹⁷ and theory,¹⁹ characterizing two-dimensional nature of the compound. Recent magnetization and neutron powder diffraction data¹⁸ showed that in the $a_m b_m$ plane, the Mn ions are ferromagnetically coupled along the $[1\bar{1}0]_m$ direction and antiferromagnetically coupled along the $[110]_m$ direction. Thus, coupling along the monoclinic b_m axis is AFM, as shown in Fig. 1. Since the AFM exchange interaction along the b_m axis is dominant compared to the interactions along

the $[1\bar{1}0]_m$ and $[110]_m$ directions, the α -NaMnO₂ is further considered as a one-dimensional AFM-chain system aligned along the b_m axis.²⁰ It is especially worth noting that the magnetic frustration is further lifted through magnetoelastic coupling effect, evidenced by a monoclinic-triclinic (P -1) structural phase transition around 45 K simultaneously with an onset of long-range AFM ordering.^{18,20}

To the best of our knowledge, there are no other theoretical reports on α -NaMnO₂ except for Refs. 16 and 19 and particularly there is no theoretical interpretation on the monoclinic-triclinic structural transition around 45 K. Different from Refs. 16 and 19, where the total energy of different phases were directly calculated, we have performed, in this paper, a first-principles study on the structural distortion of layered α -NaMnO₂. For simplicity, we confined the distortion within the ab plane considering that the interaction between MnO_2 layers stacked along the c_m axis is quite weak. We pay much attention to the distortion of Mn-Mn bond in the ab plane as well as a discussion on the distortion of

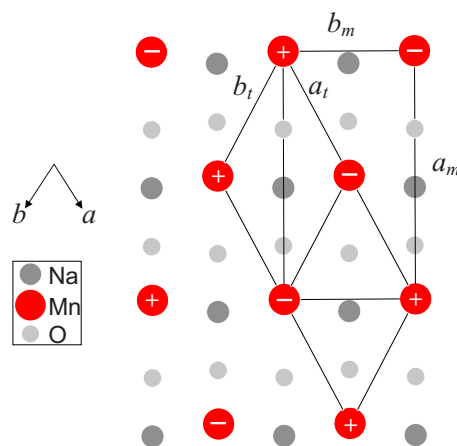


FIG. 1. (Color online) The relationship between triclinic (a_t and b_t) and monoclinic (a_m and b_m) unit cells in the ab plane of α -NaMnO₂. The symbols “+” and “-” stand for the two antiferromagnetically coupled spins.

TABLE I. Lattice parameters (\AA and $^\circ$) of triclinic (4 K) and monoclinic (300 K) phases of NaMnO_2 (Refs. 18 and 20).

Structure	a	b	c	a/b	α	β	γ
Triclinic ($P1$)	3.1677	3.1605	5.7822	1.0023	110.465	110.415	53.617
Monoclinic ($C2/m$)	5.6700	2.8550	5.8040	1.9860	90	113.230	90

MnO_6 octahedron within the MnO_2 layer. Our results show that total energy as a function of structural distortion is an effective way to clarify the phase stability among those compounds which own quite similar crystal structures.

II. COMPUTATIONAL METHOD

The self-consistent full potential linearized augmented plane-wave package WIEN2K (Ref. 21) has been employed to perform electronic-structure calculation of NaMnO_2 within the framework of density-functional theory. The muffin-tin sphere radii of Na, Mn, and O atoms are set to be 2.5 a.u., 1.9 a.u., and 1.7 a.u., respectively. The plane-wave cut-off parameters $R_{\text{MT}}K_{\text{max}}$ and G_{MAX} are 7.0 and 12.0, respectively, and the cutoff between core and valence states is -7.0 Ry. General gradient approximation (GGA) for the exchange-correlation term takes the form deduced by Perdew-Burke-Ernzerhof.²² In this study, a triclinic unit cell is adopted because of the distinct AFM ordering (Fig. 1). The monoclinic cell can be converted into the triclinic cell by: $a_t = 1/2(a_m + b_m)$ and $b_t = 1/2(a_m - b_m)$. A $1 \times 2 \times 1$ supercell containing eight atoms was used for the AFM calculation whereas a smaller $1 \times 1 \times 1$ unit cell containing four atoms was used for the FM and nonspin polarized calculations. For these two unit cells, 125 k points and 200 k points were used, respectively, in the first Brillouin zone. The self-consistency is achieved by demanding the convergence of total energy to be smaller than 1 meV. The optimization of the internal parameters shows that the site of O atoms is nearly the same as the experimental value, (0.2936, 0, and 0.7957), and the previous theoretical report for FM and AFM phases.¹⁶ Thus, the experimental internal parameters are adopted in all calculations.

III. RESULTS AND DISCUSSION

Table I lists the lattice parameters at 4 and 300 K obtained in neutron-diffraction experiments.^{18,20} Based on the relationship listed above, the monoclinic lattice parameters are equivalent to $a_t = b_t = 3.1741 \text{ \AA}$, $c_t = 5.8040 \text{ \AA}$, $\alpha = \beta = 110.627^\circ$, and $\gamma = 53.453^\circ$ in the triclinic representation. This shows that during the process of monoclinic-triclinic distortion, the isosceles triangle composed of Mn ions ($a_t = b_t \neq b_m$) is converted into random triangle ($a_t \neq b_t \neq b_m$) by lengthening one of the interchain Mn-Mn distances and shortening the other. This distortion, however, is rather small ($\sim 0.1\%$) and it is therefore expected that there is no dramatic change in total energy (E) and density of states (DOS). Figure 2 shows the E - V curves, where the value of E corresponding to the experimental volume, V_{exp} , of triclinic phase is taken as energy zero. As can be seen that the equilibrium

volume, V_0 , is derived to be larger than V_{exp} by 2.6%, showing that GGA gives a good description on the ground state. Importantly, the E - V curves of triclinic and monoclinic phases nearly overlap with each other. The very small energy difference at V_0 prohibits us from determining which phase is more stable because: (1) this difference is within the range of calculation error and (2) it originates not only from the a_t - b_t distortion but also from other parameters, such as c and angles, which contain experimental errors. Figure 2 also shows that the DOS at V_{exp} exhibit no differences between both phases. Thus, unlike the dominant stability of monoclinic phase relative to the rhombohedral phase reported earlier,¹⁶ where the E and DOS have notable differences, it is difficult to distinguish which phase is stable between triclinic and monoclinic phases.

Starting from the experimental lattice parameters (Table I), we now perform “pure” distortion calculations. We search for the possible energy minima by distorting the $a_m b_m$ ($a_t b_t$) plane of the unit cell (Fig. 1), simultaneously keeping c_m , angles and volume fixed. First, we calculate the variation in E in the a_t - b_t distortion by lengthening of a_t and contracting of b_t or vice versa (Fig. 1). In this distortion, the Mn-Mn distance along the b_m direction remains nearly unaltered, i.e., $b_m = 2.8550 \text{ \AA}$. Figure 3 shows the a_t/b_t dependence of total energy relative to the value of experimental AFM triclinic phase. The E of AFM state is significantly lower than those of the FM and nonspin polarized states, characterizing the AFM ground state. The E - a_t/b_t curves for both the FM and

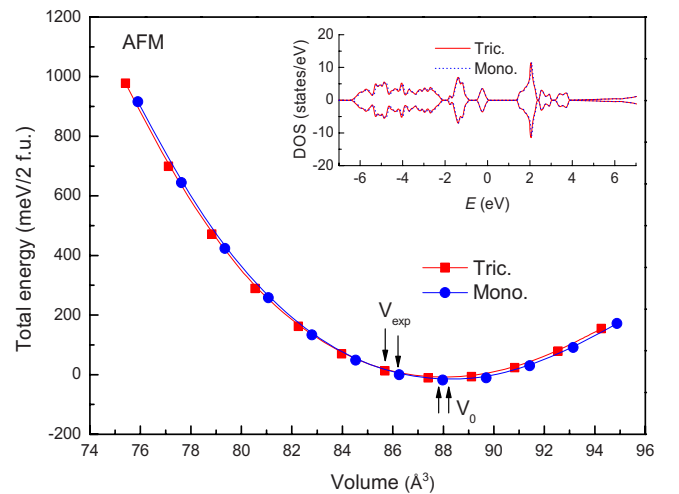


FIG. 2. (Color online) The total energy as a function of volume for both AFM triclinic and monoclinic phases. The value corresponding to the experimental volume, V_{exp} , of triclinic phase is taken as energy zero. The inset shows the DOS at V_{exp} for both phases.

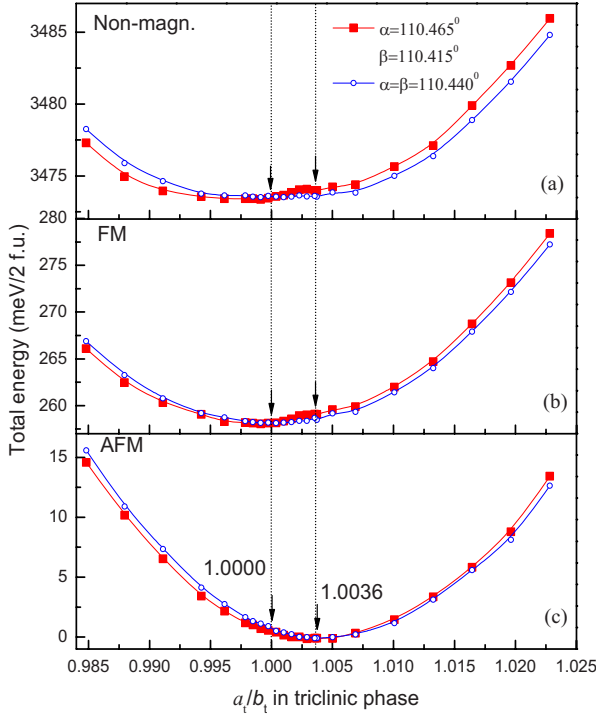


FIG. 3. (Color online) The a_t/b_t dependence of total energy for both $\alpha \neq \beta$ and $\alpha = \beta$ calculations. The value of experimental AFM triclinic volume, V_{exp} , is taken as energy zero.

nonspin polarized states are not symmetrical about $a_t/b_t = 1.0$. The curves present two local minima around $a_t/b_t = 1.0$ and 1.0036 with the former slightly lower in energy than the latter. This asymmetry might be ascribed to a slight deviation between α and β (see below). Intriguingly, the case is inverted for the AFM state. The E - a_t/b_t curve for AFM state exhibits only one minimum around $a_t/b_t = 1.0036$, close to the experimental value of $a_t/b_t = 1.0023$; both energies are found to be lower than that of $a_t/b_t = 1.0$. It is stressed here that the structure with $a_t/b_t = 1.0$ is not a monoclinic structure because α and β are not equal.

In order to illustrate more clearly the stability of monoclinic and triclinic phases, we recalculated the value of E , assuming that the angles α and β are equal and adopt the average, i.e., $\alpha = \beta = 110.440^\circ$. In this case, the distortion by lengthening of a_t and contracting of b_t is now completely equivalent to the distortion by contracting of a_t and lengthening of b_t for the FM and nonspin polarized calculations. The resultant E - a_t/b_t curve exhibits significant symmetry about $a_t/b_t = 1.0$ [Figs. 3(a) and 3(b)]. For the AFM state [Fig. 3(c)], however, the E - a_t/b_t curve with $\alpha = \beta$ presents quite similar variation as that of $\alpha \neq \beta$. The value of E at $a_t/b_t = 1.0023$ is found to be lower than that of $a_t/b_t = 1.0$ by only 1 meV, which is comparable to the calculation error. However, judging from the trend of E as a function a_t/b_t , it is safely concluded that the triclinic structure with $a_t/b_t = 1.0023$ is more stable than that of $a_t/b_t = 1.0$, which is now an exact monoclinic structure: $a = 5.6480 \text{ \AA}$, $b = 2.8540 \text{ \AA}$, $c = 5.7822 \text{ \AA}$, and $\beta = 113.034^\circ$. Hence, our result is in good agreement with recent neutron-diffraction experiments showing the ground state of AFM triclinic phase.^{18,20}

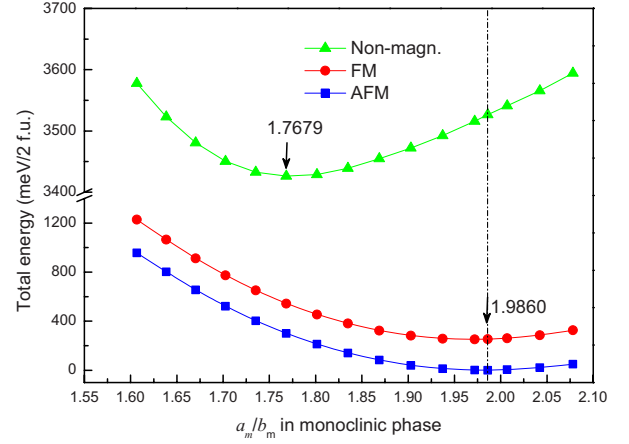


FIG. 4. (Color online) The a_m/b_m dependence of total energy relative to the value of experimental AFM monoclinic phase.

We now calculate the evolution of E as the compound undergoes structural distortion within the $a_m b_m$ plane by lengthening of a_m and contracting of b_m or vice versa (see Fig. 1). For simplicity, the calculation starts from the experimental monoclinic lattice parameters (Table I) because of its higher symmetry than that of triclinic cell. Figure 4 shows the a_m/b_m dependence of E relative to the value of experimental AFM monoclinic phase. In the nonspin polarized calculation, there exists a minimum around $a_m/b_m = 1.7679$, much close to the idea value of 1.7320 . This could be attributed to higher geometrical symmetry of $a_m/b_m = 1.7320$, at which Mn ions form equilateral triangles in the $a_m b_m$ plane and all the Mn-Mn distances become equal to each other (note that this is not the rhombohedral structure because the MnO_6 octahedra are still distorted). As spin polarization is involved in the distortion, however, the value of E decreases rapidly and its minimum now moves to higher value of $a_m/b_m = 1.9860$, pointing exactly to the experimental monoclinic structure (see Table I). This shows that introduction of magnetic Mn^{3+} ions, either in FM or AFM ordering, tends to distort the geometrical crystal structure from equilateral to isosceles triangle, showing a magnetoelastic effect. Figure 4 also shows that the AFM state has a lower E than the FM state. Thus, our results not only show that the AFM state is stable compared to the FM and nonspin polarized states, in good agreement with previous report¹⁶ where the total energies as a function of volume for different phases were directly calculated but also predict the right value of a_m/b_m , which is originated from the magnetoelastic coupling.

Based on the results presented above, our study on structural distortions predicts right AFM triclinic ground state. The calculated ratio of lattice parameters, a_t/b_t (a_m/b_m) of triclinic (monoclinic) phase is also much close to the experimental result. In reality, there are many systems whose different possible crystallographic structures are so similar to each other so that it is difficult to distinguish which is the ground state based on conventional total energy and DOS. Our calculations indicate that evolution of total energy with structural distortion is an effective way to clarify the phase stability of these systems.

In addition to these predictions, it is interesting to compare the a_m - b_m and a_t - b_t distortions. From a viewpoint of

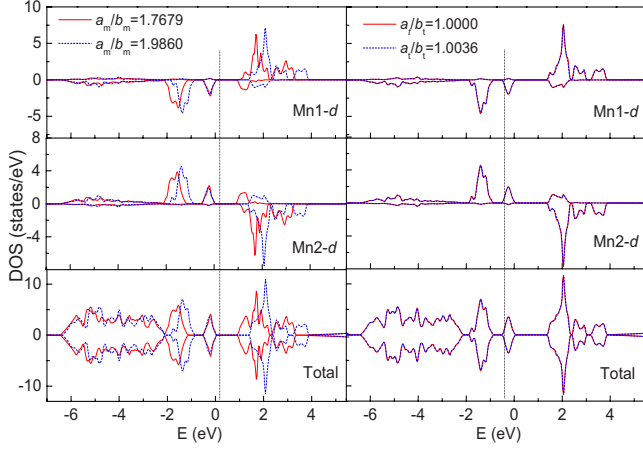


FIG. 5. (Color online) The total and projected DOS at $a_m/b_m = 1.7679$ and 1.9860 for the a_m - b_m distortion (left panel) and at $a_t/b_t = 1.0$ and 1.0036 for the a_t - b_t distortion with $\alpha = \beta = 110.440^\circ$ (right panel).

pure geometry, as an equilateral triangle consisting of Mn ions is distorted into an isosceles triangle with $a_t = b_t \neq b_m$ (i.e., monoclinic), and further distorted into a random triangle with $a_t \neq b_t \neq b_m$ (i.e., triclinic), the symmetry is reduced in sequence. Such a reduction in symmetry can be readily induced by magnetism, as clearly illustrated in Figs. 3 and 4. In the a_m - b_m distortion, both FM and AFM ordering can induce a distortion from an equilateral to an isosceles triangular alignment of Mn ions, accompanying a large variation in distortion-related energy due to the strong magnetoelastic coupling. On the contrary, in the a_t - b_t distortion, the FM ordering does not induce a distortion from an isosceles to a random triangular alignment of Mn ions. The monoclinic-triclinic distortion can be only induced by AFM ordering, accompanying a small variation in distortion-related energy. This strongly suggests that magnetoelastic coupling is quite weak and the interchain AFM frustration is further lifted by this tiny a_t - b_t distortion, ultimately prompting the formation of long-range AFM ordering in low temperatures.^{18,20}

Differences between the a_m - b_m and a_t - b_t distortions can be further understood by DOS as shown in Fig. 5. For the experimental monoclinic phase with $a_m/b_m = 1.9860$ (Table I), the Mn-O-Mn bond angles within the MnO_2 layer are nearly 90° , giving rise to quite narrow Mn $3d$ bands. The t_{2g} state is located between -1.6 and -1.0 eV for the Mn1 majority spin. A bandgap of 1.3 eV separates well the $d_{3z^2-r^2}$ and $d_{x^2-y^2}$ bands due to the Jahn-Teller distortion, similar to the report in Ref. 19. In the a_m - b_m distortion, the average distortion of MnO_6 octahedron defined by d_1/d_2 , where d_1 and d_2 are the long and short Mn-O bond lengths, respectively, is increased from 17% ($d_1 = 2.3114$ Å and $d_2 = 1.9701$ Å) at $a_m/b_m = 1.7679$ to 24% ($d_1 = 2.3947$ Å and $d_2 = 1.9284$ Å) at $a_m/b_m = 1.9860$, accompanied by a large bandgap broadening of about 0.5 eV. Such a large distortion favors the ferro-orbital ordering of $d_{3z^2-r^2}$ orbital along the long-bond direction of MnO_6 octahedron.¹⁸

In the a_t - b_t distortion, the total and projected DOS for both monoclinic ($a_t/b_t = 1.0$) and triclinic ($a_t/b_t = 1.0036$ and

$\alpha = \beta = 110.440^\circ$) phase are nearly overlap with each other. However, a careful scrutiny still reveals a quite small bandgap broadening of about 0.008 eV after the distortion. With such a small modification in DOS, there are no significant changes in the occupation of d orbitals, the Mn-O bond lengths, and the Mn-O-Mn bond angles. Indeed, the spin moment of Mn is derived to be $3.30 \mu_B/\text{Mn}$ for both phases. In the distortion, the four short Mn-O bonds ($d_2 = 1.9270$ Å) at $a_t/b_t = 1.0$ split into two unequal bonds ($d_2 = 1.9244$ and 1.9296 Å) at $a_t/b_t = 1.0036$ but the two long Mn-O bonds ($d_1 = 2.3829$ Å) remain nearly unaltered. The resultant average distortion is nearly unchanged, i.e., $d_1/d_2 = 24\%$. Hence, the reduction in symmetry of MnO_6 octahedron is induced only by the four short Mn-O bonds, different from the a_m - b_m distortion where both the long and the short Mn-O bonds are elongated. It might be this short-bond related energy that causes the tiny monoclinic-triclinic transition.

Finally, it might be reasonable to assume that the distortion-associated energy correlates to magnetic exchange interactions. In the a_m - b_m distortion, Mn-Mn bond length varies considerably along the b_m direction, giving rise to a relatively larger variation in energy because of the strong intrachain AFM coupling along this axis. On the contrary, in the a_t - b_t distortion, the Mn-Mn bond length along b_m direction remains nearly unaltered, i.e., 2.8550 Å, leading to a relatively smaller variation in energy because of the weak interchain interaction. It was recently reported^{18,20} that the AFM interaction along the b_m axis is much larger in magnitude than those along the a_t and b_t directions because of the cooperative ferro-orbital ordering of $d_{3z^2-r^2}$ orbital in the distorted MnO_6 octahedra. Thus, our results are qualitatively consistent with strong anisotropic exchange interactions of this material.

IV. CONCLUSIONS

In summary, we have performed a first-principles study on the structural distortion of frustrated antiferromagnet α - NaMnO_2 by assuming that the triangle consisting of Mn ions is distorted along the a_t and b_t directions in the triclinic cell and along the a_m and b_m directions in the monoclinic cell, respectively. Both distortions exhibit quite different behavior. The energy variation in the a_t - b_t distortion is much smaller than that in the a_m - b_m distortion, which might be related to the anisotropic exchange interactions. Our calculation predicts the correct ratio of lattice parameters, a/b , in triclinic and monoclinic phases and qualitatively explains that AFM triclinic phase is the desired ground state, whose origin is the magnetoelastic effect lifting the magnetic frustration. Thus, our study on structural distortion is an effective way to clarify the phase stability among those compounds which own quite similar crystal structures.

ACKNOWLEDGMENTS

This work is supported by Scientific Research Foundation for Returned Scholars (Grant No. 0124012014), Huazhong University of Science and Technology.

*Corresponding author; zwouyang@mail.hust.edu.cn

- ¹A. R. Armstrong and P. G. Bruce, *Nature (London)* **381**, 499 (1996).
- ²I. Terasaki, Y. Sasago, and K. Uchinokura, *Phys. Rev. B* **56**, R12685 (1997).
- ³M. Winter, J. O. Besenhard, M. E. Spahr, and P. Novák, *Adv. Mater.* **10**, 725 (1998).
- ⁴Y. Y. Wang, N. S. Rogado, R. J. Cava, and N. P. Ong, *Nature (London)* **423**, 425 (2003).
- ⁵K. Takada, H. Sakurai, E. Takayama-Muromachi, F. Izumi, R. A. Dilanian, and T. Sasaki, *Nature (London)* **422**, 53 (2003).
- ⁶M. L. Foo, Y. Wang, S. Watauchi, H. W. Zandbergen, T. He, R. J. Cava, and N. P. Ong, *Phys. Rev. Lett.* **92**, 247001 (2004).
- ⁷S. K. Mishra and G. Ceder, *Phys. Rev. B* **59**, 6120 (1999).
- ⁸M. V. Mostovoy and D. I. Khomskii, *Phys. Rev. Lett.* **89**, 227203 (2002).
- ⁹C. A. Marianetti, D. Morgan, and G. Ceder, *Phys. Rev. B* **63**, 224304 (2001).
- ¹⁰C. Darie, P. Bordet, S. de Brion, M. Holzzapfel, O. Isnard, A. Lecchi, J. E. Lorenzo, and E. Suard, *Eur. Phys. J. B* **43**, 159 (2005).
- ¹¹T. Jia, G. Zhang, Z. Zeng, and H. Q. Lin, *Phys. Rev. B* **80**, 045103 (2009).
- ¹²M. Hemmida, H.-A. Krug von Nidda, N. Büttgen, A. Loidl, L. K. Alexander, R. Nath, A. V. Mahajan, R. F. Berger, R. J. Cava, Y. Singh, and D. C. Johnston, *Phys. Rev. B* **80**, 054406 (2009).
- ¹³J. P. Parant, R. Olazcuaga, M. Devalette, C. Fouassier, and P. Hagenmuller, *J. Solid State Chem.* **3**, 1 (1971).
- ¹⁴V. M. Jansen and R. Hoppe, *Z. Anorg. Allg. Chem.* **399**, 163 (1973).
- ¹⁵R. Hoppe, G. Brachtel, and M. Jansen, *Z. Anorg. Allg. Chem.* **417**, 1 (1975).
- ¹⁶O. I. Velikokhatnyi, C.-C. Chang, and P. N. Kumta, *J. Electrochem. Soc.* **150**, A1262 (2003).
- ¹⁷A. Zorko, S. El Shawish, D. Arcon, Z. Jaglicic, A. Lappas, H. van Tol, and L. C. Brunel, *Phys. Rev. B* **77**, 024412 (2008).
- ¹⁸M. Giot, L. C. Chapon, J. Androulakis, M. A. Green, P. G. Radaelli, and A. Lappas, *Phys. Rev. Lett.* **99**, 247211 (2007).
- ¹⁹G. R. Zhang, L. J. Zou, Z. Zeng, and H. Q. Lin, *J. Appl. Phys.* **105**, 07E512 (2009).
- ²⁰C. Stock, L. C. Chapon, O. Adamopoulos, A. Lappas, M. Giot, J. W. Taylor, M. A. Green, C. M. Brown, and P. G. Radaelli, *Phys. Rev. Lett.* **103**, 077202 (2009).
- ²¹P. Blaha, K. Schwarz, G. Madsen, D. Kvasnicka, and J. Luitz, *WIEN2K* (Technische Universität Wien, Austria, 2007).
- ²²J. P. Perdew, K. Burke, and M. Ernzerhof, *Phys. Rev. Lett.* **77**, 3865 (1996).